Correlations of Crystal Structures of DNA Oligonucleotides with Enantioselective Recognition by $Rh(phen)_2phi^{3+}$: Probes of DNA Propeller Twisting in Solution†

Donna Campisi, Takashi Morii,‡ and Jacqueline K. Barton*

Division of Chemistry and Chemical Engineering, California Institute of Technology, Pasadena, California 91125

Received November 4, 1993; Revised Manuscript Received January 27, 1994®

ABSTRACT: $Rh(phen)_2phi^{3+}$ (phen = 1,10-phenanthroline; phi = 9,10-phenanthrenequinone diimine) avidly binds to DNA *via* intercalation from the major groove and upon photoactivation produces strand scission with single base 5′ asymmetry. Enantiomers of $Rh(phen)_2phi^{3+}$, which lack hydrogen-bonding substituents in ancillary positions, distinguish a DNA site through shape-selection; site recognition depends upon the local variations in structure at a binding site. Here, we examine the application of Δ-$Rh(phen)_2phi^{3+}$ as a sequence-dependent structural probe and, in particular, as a probe of DNA propeller twisting in solution, by comparing directly cleavage results using Δ- and Λ-$Rh(phen)_2phi^{3+}$ on crystallographically characterized oligonucleotides with several sequence-dependent crystallographic parameters. The three oligonucleotides examined in this study are the Dickerson–Drew dodecamer, 5′-CGCGAATTCGCG-3′, the *Nar* I dodecamer, 5′-ACCGGCGCCACA-3′, and the CG decamer, 5′-CCAACGTTGG-3′, all of which have been crystallized in the B-form. Enantioselective cleavage and reaction favored by the Δ-isomer is found to be governed locally by the opening of the site in the major groove. A correlation is demonstrated between cleavage by Δ-$Rh(phen)_2phi^{3+}$ and the opening in the major groove that results from the change in propeller twist (differential propeller twist) at a base step. When the major groove is closed as a result of a change in propeller twist, there is little cleavage evident by either enantiomer; at sites which are indicated crystallographically to be open in the major groove, a direct correlation is observed between enantioselective cleavage and the degree of opening. A trend of higher enantioselectivity at sites possessing higher twist angles is also observed. The roll angle of a site in isolation, the rise per base step, and the groove width show no correlation with cleavage. The distribution of reaction products at a site, as a result of partitioning along oxygen-dependent or oxygen-independent pathways, also provides a sensitive measure of the shape-complementarity between metal complex and binding site. These results provide evidence for site-recognition by the metal complex which correlates directly with DNA propeller twisting in oligonucleotide crystals. Importantly, these results indicate that $Rh(phen)_2phi^{3+}$ may be uniquely applied as a chemical probe for sequence-dependent changes in the propeller twisting of DNA.

Although high-resolution crystallographic structures of DNA oligonucleotides have been available for over a decade [for reviews, see Kennard and Hunter (1989) and Drew et al. (1990)], the rules by which sequence encodes the three-dimensional structure of duplex DNA are far from understood. Understanding the relationship between the one-dimensional sequence of DNA and its three-dimensional structure is essential in order to decipher how proteins recognize DNA sequence-specifically and how one might rationally design new chemotherapeutic agents which target specific DNA sites. The structures of protein–DNA complexes, elucidated using X-ray crystallography, have pointed to DNA conformation as one factor influencing recognition (Pabo & Sauer, 1992; Steitz, 1990). Base pairs which are not contacted directly by protein side chains have been shown to have a significant effect on binding affinity. Indirect readout, where protein side chains interact specifically with the local twists and turns of the phosphate backbone rather than through direct hydrogen-bonding interactions with the base pairs, may be a prevalent theme in protein–nucleic acid interactions (Otwinowski et al., 1988). Studies of shape-selective recognition of DNA by small molecules have also underscored the importance of shape-recognition without hydrogen bonding in effecting site-specificity (Pyle & Barton, 1990; Sitlani & Barton, 1993).

Few techniques are available to probe local, sequence-dependent variations in nucleic acid structure in solution. High-resolution NMR studies now provide methods to examine oligonucleotide structure in solution, but investigations are often restricted to tests of self-complementary oligomers with lengths of 14 base pairs or fewer (Patel et al., 1987). Moreover, detailed information, particularly with regard to the disposition of bases, is often obtained with confidence only in studies with a bound drug or DNA-binding peptide. Thus, in order to examine the sequence-dependent variations in structure of long DNA fragments in solution, the development of small chemical and enzymatic probes for nucleic acid structure becomes essential (Tullius, 1992; Sigman, 1986; Drew & Travers, 1984; Chow & Barton, 1992). Results from such studies are still more powerfully interpreted when comparative studies are conducted on crystallographically characterized structures.

Our laboratory has developed a novel probe of DNA propeller twisting based upon enantioselective recognition of DNA by the metallointercalators, Λ- and Δ-$Rh(phen)_2phi^{3+}$ (phen = 1,10-phenanthroline; phi = 9,10-phenanthrenequinone diimine). The propeller twisting of DNA, first observed by high-resolution crystallography, is difficult to characterize in solution by NMR methods (Pardi et al., 1988; Metzler et al., 1990; Nerdal et al., 1989; Kaluarachchi et al, 1991). How propeller twisting varies as a function of sequence and how

† We are grateful to the National Institutes of Health (GM33309 and an NRSA predoctoral traineeship to D.C.) for their financial support.

* To whom correspondence should be addressed.

‡ Present address: Department of Polymer Science and Engineering, Kyoto Institute of Technology, Kyoto 606, Japan.

® Abstract published in *Advance ACS Abstracts,* March 15, 1994.

0006-2960/94/0433-4130$04.50/0

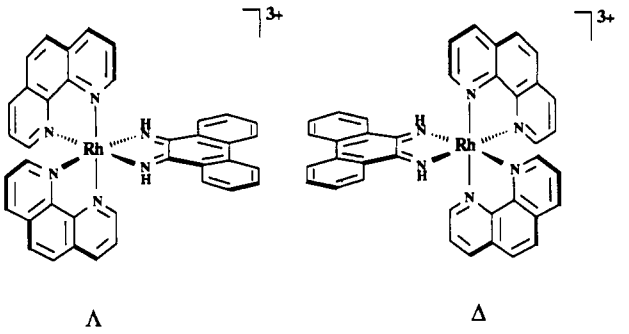

such sequence-dependent variations may be exploited in strategies for recognition are interesting issues to consider. $Rh(phen)_2phi^{3+}$, our probe of DNA propeller twists (Pyle et al., 1990a), binds DNA avidly by intercalation and, with photoactivation, promotes strand cleavage directly at its site of binding (Pyle et al., 1989; Sitlani et al., 1992). Two-dimensional NMR experiments demonstrate that the complex intercalates from the major groove through stacking of the phi ligand (David & Barton, 1993).

Several structural features of $Rh(phen)_2phi^{3+}$ contribute to its usefulness as a shape-selective probe of DNA conformation. The complex is coordinatively saturated and inert to substitution; hence, all interactions with DNA are noncovalent. The wide atomic surface of the phi ligand permits intimate association with DNA via intercalation. However, the ancillary phenanthroline ligands of $Rh(phen)_2phi^{3+}$ provide steric constraints. Specifically, within an intercalation site with base pairs stacked nearly perpendicular to the helix axis, steric collisions should occur between the overhanging 2,9 hydrogens of the phenanthrolines and the base pairs. At sites having less steric interference in the major groove owing to propeller twisting or tilting, for example, intercalation by $Rh(phen)_2phi^{3+}$ is made facile. Thus, the site-selectivity of $Rh(phen)_2phi^{3+}$ may be understood based upon *shape-selection*. Indeed, no hydrogen-bonding functionalities are present on the ancillary ligands of the complex. Because of these same structural characteristics, $Rh(phen)_2phi^{3+}$ shows no cleavage on A-like double helical regions of RNA but targets specifically sites of tertiary interaction in folded RNA molecules where the major groove is opened and accessible (Chow et al., 1992a).

The potential applicability of $Rh(phen)_2phi^{3+}$ in probing DNA propeller twisting became apparent in comparing the sequences cleaved by $Rh(phen)_2phi^{3+}$ enantiomers on a series of restriction fragments (Pyle et al., 1990a). Resolution of $Rh(phen)_2phi^{3+}$ into its Δ- and Λ-enantiomers provides discrete structural probes whose difference in cleavage necessarily depends only upon binding properties. Overall binding and cleavage are generally greater for the Δ-isomer of metallointercalators on right-handed DNA helices (Barton, 1986). Δ- and Λ-$Rh(phen)_2phi^{3+}$ both cleave modestly at 5′-N*Y*YN-3′ steps, (where the italic Y denotes the site of cleavage), and neither show appreciable cleavage at 5′-N*R*YN-3′ steps.[1] However, at 5′-Y*Y*RN-3′ steps, there is substantial cleavage by Δ-$Rh(phen)_2phi^{3+}$ but not by the Λ-enantiomer. Strikingly, those sites which are cleaved preferentially were found to be those which are characterized by a high degree of differential propeller twist.[2] Thus, these results suggested that the shape-selective metal complex might serve to recognize and distinguish propeller-twisted DNA sites in solution on the basis of matching shape and symmetry. Figure 1 schematically summarizes the basis for this proposed enantioselective discrimination at propeller twisted sites.

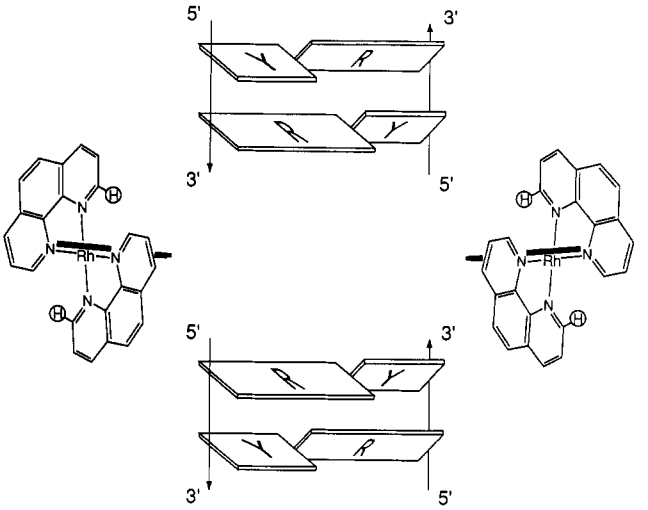

FIGURE 1: Schematic representation of enantiomeric discrimination in binding by Λ-(left) and Δ-$Rh(phen)_2phi^{3+}$ (right) as a probe of DNA propeller twisting. 5′-YR-3′ (top) and 5′-RY-3′ (bottom) steps are viewed from the major groove. The phi ligand (heavy line) of the enantiomers is oriented into the page for intercalative binding. Intercalation by the octahedral metal complex at canonical DNA base steps yields steric clashes between the 2,9 hydrogens (circled) of $Rh(phen)_2phi^{3+}$ and the bases, unless the local conformation leads to an opening in the major groove. Differential propeller twisting at 5′-YR-3′ steps provides an opening in the major groove for the Δ-isomer; in contrast, there are clashes at this step between the phenanthroline ancillary ligands and the pyrimidine bases for the Λ-isomer. At the 5′-RY-3′ step, neither enantiomer may bind with facility since there are clashes between the larger purines and the ancillary ligands of both enantiomers; the major groove is closed.

Variations in DNA reactivity have also been found to be governed by subtle considerations of shape. The analysis of oligonucleotide products after photocleavage by $Rh(phen)_2phi^{3+}$ has been consistent with a DNA cleavage mechanism which involves direct abstraction of the C3′-hydrogen atom by the photoexcited, intercalated phi ligand (Sitlani et al., 1992). The products obtained as a function of oxygen concentration indicated a partitioning of the reaction along two pathways following abstraction of the C3′-hydrogen atom (Stubbe & Kozarich, 1987). The oxygen-independent pathway leads to the production of 5′- and 3′-phosphate termini with the release of free nucleic acid bases. The oxygen-dependent pathway yields a 5′-phosphate terminus and a 3′-phosphoglycaldehyde terminus with the release of base propenoic acids. Differences in partitioning between the pathways as a function of sequence and by the two enantiomers therefore provides an additional measure of the complementarity in shape of the complex with the shape of its binding site.

In order to develop $Rh(phen)_2phi^{3+}$ recognition and reaction as a sensitive probe of DNA structure in solution, this work examines quantitatively on crystallographically characterized oligomers the correlation between enantioselectivity in cleavage by $Rh(phen)_2phi^{3+}$ with sequence-dependent differential propeller twisting. Correlations with other structural parameters as a function of sequence are considered as well. Three crystallographically characterized oligonucleotides were examined in solution using Δ- and Λ-$Rh(phen)_2phi^{3+}$: (i) the Dickerson–Drew dodecamer (Dickerson & Drew, 1981; Drew et al., 1981; Fratini et al., 1982); (ii) the *Nar* I dodecamer (Timsit et al., 1989); and (iii) the CG decamer (Privé et al.,

[1] Abbreviations: Y denotes pyrimidine; R denotes purine; N denotes any base.

[2] We define differential propeller twist as the angle between the two purine bases projected onto the plane defined by the dyad and helical axes.

1991).

Dickerson–Drew:	5′-CGCGAATTCGCG-3′ 3′-GCGCTTAAGCGC-5′
Nar I:	5′-ACCGGCGCCACA-3′ 3′-TGGCCGCGGTGT-5′
CG decamer:	5′-CCAACGTTGG-3′ 3′-GGTTGCAACC-5′

These oligonucleotides were chosen because each crystallizes in the B-form and each packs differently in the crystal. We report here a significant correlation between enantioselectivity of cleavage by $Rh(phen)_2phi^{3+}$ and the local conformation of the base step as obtained from crystallographic parameters in the absence of metal complex. Additionally, the reactivity of the complex within a site appears to be influenced directly by the sequence-dependent variations in local conformation. These parameters therefore provide a foundation for applying $Rh(phen)_2phi^{3+}$ enantiomers in probing sequence-dependent variations in structure in solution.

MATERIALS AND METHODS

Materials. Oligonucleotides were synthesized via the phosphoramide method (Caruthers et al., 1987) using 1.0 μM columns on an ABI 391 DNA–RNA synthesizer. A reversed-phase, C18 Dynamax column was used on a Waters HPLC for the purification of DNA. Labeling reactions were accomplished with γ^{32}P-ATP (NEN) and polynucleotide kinase. Labeled oligonucleotides were purified using Nensorb columns and stored dry at 4 °C. For non-self-complementary oligonucleotides, equimolar concentrations of each strand were heated together to 90 °C and cooled over several hours to allow proper annealing to occur. $Rh(phen)_2phi^{3+}$ was synthesized as previously described (Pyle et al., 1990b). Enantiomers were resolved by column chromatography with a chiral eluent (David & Barton, 1993). Quantitation of metal concentrations was accomplished using a CARY 219 (Varian) spectrometer, based on $\epsilon(362) = 19\,400\ M^{-1}\ cm^{-1}$.

Photocleavage Reactions. Reactions contained 480 μM nucleotides, 50 mM sodium cacodylate buffer pH 7.0, and 25 μM rhodium complex and were irradiated at 313 nm with a 1000-W Hg–Xe lamp and monochromator. Irradiation times were typically 4.5 min. Different irradiation times yielded the same distribution of cleavage, although the total amount cleaved was increased with longer irradiation. After photocleavage, an aliquot of each reaction mixture was taken and dried in vacuo. These aliquots, along with Maxam–Gilbert sequencing reactions (Maniatis et al., 1982) and controls, were then taken up in a NaOH–formamide dye, heated to 90 °C for 3 min, chilled on ice for 1 min, and loaded on a 20%/8.3 M urea polyacrylamide gel. Gels were eluted about 4 h at 1600 V. Upon completion, gels were wrapped and exposed to a phosphorimaging plate for 12 h. These plates were scanned on a Molecular Dynamics phosphorimager.

Quantitation of Cleavage. Gel electrophoresis experiments were quantified using Molecular Dynamics ImageQuant software. DNA was irradiated in the absence of metal (light control) to provide a control for damage due to irradiation. Cleavage at each base was corrected for any damage shown in this light control as follows

$$c_{corr,i} = \left(\frac{x}{c_{tot}}\right)c_i - \left(\frac{x}{h_{tot}}\right)h_i \qquad (1)$$

where $c_{corr,i}$ is the corrected value of a cleavage band, c_i is the uncorrected integration volume of a cleavage band, h_i is the value of the corresponding band in the light control, c_{tot} and h_{tot} are the total number of counts in the cleavage and light control lanes, respectively, and x is a factor arbitrarily set to 10 million counts which allows comparison of sites in non-self-complementary strands (which are corrected to different light control values.)

After this correction was made for Λ and Δ cleavage at each position, a normalization which allows for comparison between experiments was performed. The Δ cleavage for each experiment was normalized to 4% for self-complementary oligonucleotides. For the *Nar* I dodecamer, cleavage was normalized so that corrected Δ cleavage from both strands added together represented 8% of the uncut material. This correction was accomplished to preserve any reactivity differences present between the two strands. Λ cleavage was also normalized to 4% Δ cleavage, thus leaving enantioselectivities (Δ/Λ) unaffected by the normalization. Actual percent cleaved was varied to establish such variations did not affect the distribution of cleavage intensities.

The total cleavage at each *base* was then obtained by adding together 3′-phosphate and 3′-phosphoglycaldehyde termini observed on the gel. The amount of cleavage at each intercalation site is best represented as a sum of cleavage from each strand. Thus, total cleavage at each base step was obtained by adding together the corrected cleavage on both strands to the 5′ side across the intercalation site. This summation is necessary since cleavage may occur on either strand. Cleavage intensities are added in the 5′-direction because in general photoactivation of $Rh(phen)_2phi^{3+}$ promotes cleavage with single base 5′-asymmetry, that is, the C3′-hydrogen atom of the deoxyribose to the 5′-side of the intercalation site appears to be preferentially abstracted (Sitlani et al., 1992).

Calculation of Differential Propeller Twisting, x_p. There are two parameters which describe the rotation of a base pair/step about its long axis. Propeller twist (ω) is the angle at which the bases in a base pair twist with respect to one another, roll (ρ) is the angle which describes the angle between the mean plane of the first base pair in a base step with the mean plane of the second base pair of that step. Both parameters then contribute to a base step opening or closing toward the major groove. This opening may be approximated as the angle between purine planes (neglecting helical twist), as shown in Figure 2. For each of the four base steps, the calculation of this angle differs. However, the roll angle is added in all cases. The expressions are given as follows:

$$\text{for the 5′-YR-3′ step,}\quad x_p = a + b + \rho \qquad (2)$$

$$\text{for the 5′-RY-3′ step,}\quad x_p = -(a + b) + \rho \qquad (3)$$

$$\text{for the 5′-YY-3′ step,}\quad x_p = (a - b) + \rho \qquad (4)$$

$$\text{for the 5′-RR-3′ step,}\quad x_p = (b - a) + \rho \qquad (5)$$

where a is half the propeller twisting value (ω) at the 5′ side of the base step and b is half the ω value at the 3′ side of the base step. The parameters a, b, and ω are all negative by convention (EMBO Workshop on DNA Curvature and Bending, 1989). Just as a negative roll angle describes major groove opening, a negative x_p value also describes major groove opening. It may be seen that for a 5′-YR-3′ step, the greater the propeller twisting, the greater the major groove opening, whereas for a 5′-RY-3′ step, the greater the propeller twisting, the more closed the major groove becomes.

All values for ω and γ were taken from the referenced crystallographic parameters. Differential propeller twist angle

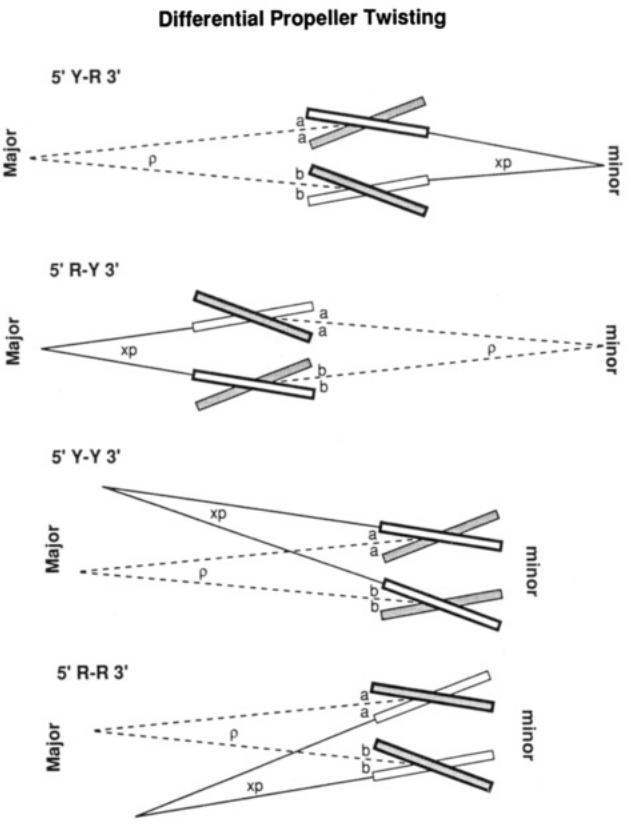

FIGURE 2: Geometrical projections of each of the four base steps. The view is along the long aix of the base pairs, with the major groove to the left side of the projection and the minor groove to the right side. The purines are shown in white and the pyrimidines in gray. The front strand is in the 3′–5′ direction and is represented by thick outlines. The back strand is in the 5′–3′ direction and is represented by thin outlines. Roll (ρ) and x_p angles show the direction of opening.

neglecting roll angle, $x_p$nr, was also calculated as a comparison. Errors for x_p and $x_p$nr, when included, are represented by the range of values calculated using both ends of a self-complementary but nonsymmetrical crystal structure (Dickerson & Drew, 1981).

RESULTS

General Features of Photocleavage by Rh(phen)$_2$phi^{3+}

Cleavage by Δ- and Λ-Rh(phen)$_2$phi^{3+} differs in position, intensity, and partitioning between reaction pathways. Autoradiograms of polyacrylamide gels which indicate sites of cleavage on all three oligonucleotides are shown in Figure 3, and the results are quantitated in Table 1. For all three oligonucleotides, the cleavage by the racemic mixture shows characteristics of both enantiomers, with more similarity to that of the Δ enantiomer.

Dickerson–Drew Dodecamer. In the Dickerson–Drew dodecamer, Δ-Rh(phen)$_2$phi^{3+} cleaves predominantly at C_9, with a lesser amount of cleavage at the C_3 which is across from C_9 at the same base step (Figure 3A). There is also a moderate amount of cleavage at the T_8 site by the Δ enantiomer. The Λ enantiomer, however, shows a similar amount of cleavage at the T_8 and C_9 sites.

Nar I Dodecamer. This oligonucleotide contains two intercalation sites which display enantioselective cleavage. As can be seen in Figure 3B, at both cytosines at the C_3 site, C_3 and C_{21}, Δ-Rh(phen)$_2$phi^{3+} cleaves significantly more than the Λ-isomer. At the C_9-T_{15} intercalation site, cleavage by the Δ enantiomer is greater than that of Λ for C9 but equivalent at T_{15}. Δ- and Λ-Rh(phen)$_2$phi^{3+} cleave at C_6 and C_{18} to a similar extent, although it is a 5′-YR-3′ step. This cleavage is less than that seen for the Δ-isomer at the two more highly enantioselective sites.

CG Oligonucleotide. There is one highly enantioselective cleavage site for Δ-Rh(phen)$_2$phi^{3+} on this oligonucleotide, as shown in Figure 3C. At C_5 Δ cleaves more than Λ by a factor of 6. The second strongest site for the Δ enantiomer, T_8, is cleaved almost equally by the Λ enantiomer.

Asymmetry of Photocleavage

In addition to cleavage position, the 5′ asymmetry associated with cleavage also provides information as to how these complexes are bound to DNA. Of the four strongest cleavage sites for Δ-Rh(phen)$_2$phi^{3+}, two, C_9-C_3 on the Dickerson–Drew dodecamer and C_9-T_{15} on the *Nar I* dodecamer, show an appreciable asymmetry in the extent of cleavage at each side of the site, as shown in Table 1. (For the center of the self-complementary CG oligonucleotide, this asymmetry cannot be determined.) In the case of the Dickerson–Drew dodecamer, C_9 strikingly yields about 23 times as much cleavage as the corresponding C_3, and for the *Nar* I oligonucleotide, C_9 is cleaved about 9 times as strongly as the corresponding T_{15}. These two sites correspond to 5′-*YY*R-3′ steps. We ascribe this asymmetry to the canting of the molecule in the site to one strand (Sitlani et al., 1992).

Not every 5′-YR-3′ step shows appreciable asymmetry in cleavage by Rh(phen)$_2$phi^{3+}. A 5′-CA-3′ step examined earlier (Sitlani et al., 1992) in the context of 5′-GCAT-3′ does not show appreciable asymmetry for the racemic complex, and the central 5′-GCGC-3′ of the *Nar* I dodecamer similarly does not show asymmetry for the Δ-, Λ-, or racemic complexes.

These observations indicate that flanking sequence may have an influence over the manner in which the complex binds to a site. That is, generally speaking, the complex cleaves preferentially at a 5′-YR-3′ step which has a pyrimidine to the 5′-side of that step. If only one side has a flanking pyrimidine, cleavage by the complex appears to be skewed toward that side. If the step is flanked on the 5′-side of both bases by pyrimidines, there is not as much asymmetry in cleavage, but the overall cleavage is still high, whereas if the step is flanked on both sides by purines, the apparent canting and cleavage tend to be lower.

Correlation of Enantioselectivity with Major Groove Opening

Both enantioselectivity and absolute cleavage by the Δ-isomer show correlations with differential propeller twisting. This correlation between differential propeller twist and cleavage by Δ-Rh(phen)$_2$phi^{3+} is plotted in Figure 4. Shown are plots of cleavage by Δ-Rh(phen)$_2$phi^{3+} versus differential propeller twisting with and without contributions of roll. It can be seen that at positive values for x_p, where the major groove is closed, the amount of Δ cleavage is low. However, when the major groove is open, values for cleavage by Δ-Rh(phen)$_2$phi^{3+} are substantially higher. These sites all correspond to 5′ Y–R 3′ steps.

An important exception is found in 5′-$G_5C_6G_7$-3′ in the *Nar* I dodecamer which shows little cleavage. Although strongly propeller twisted in the crystal structure, this site appears to show anomalously low cleavage and enantioselectivity. It is interesting that in this segment of the oligonucleotide in the crystal two helices are packed closely against one another. It is likely that this type of packing has a deforming effect in the crystal in this region of the helix.

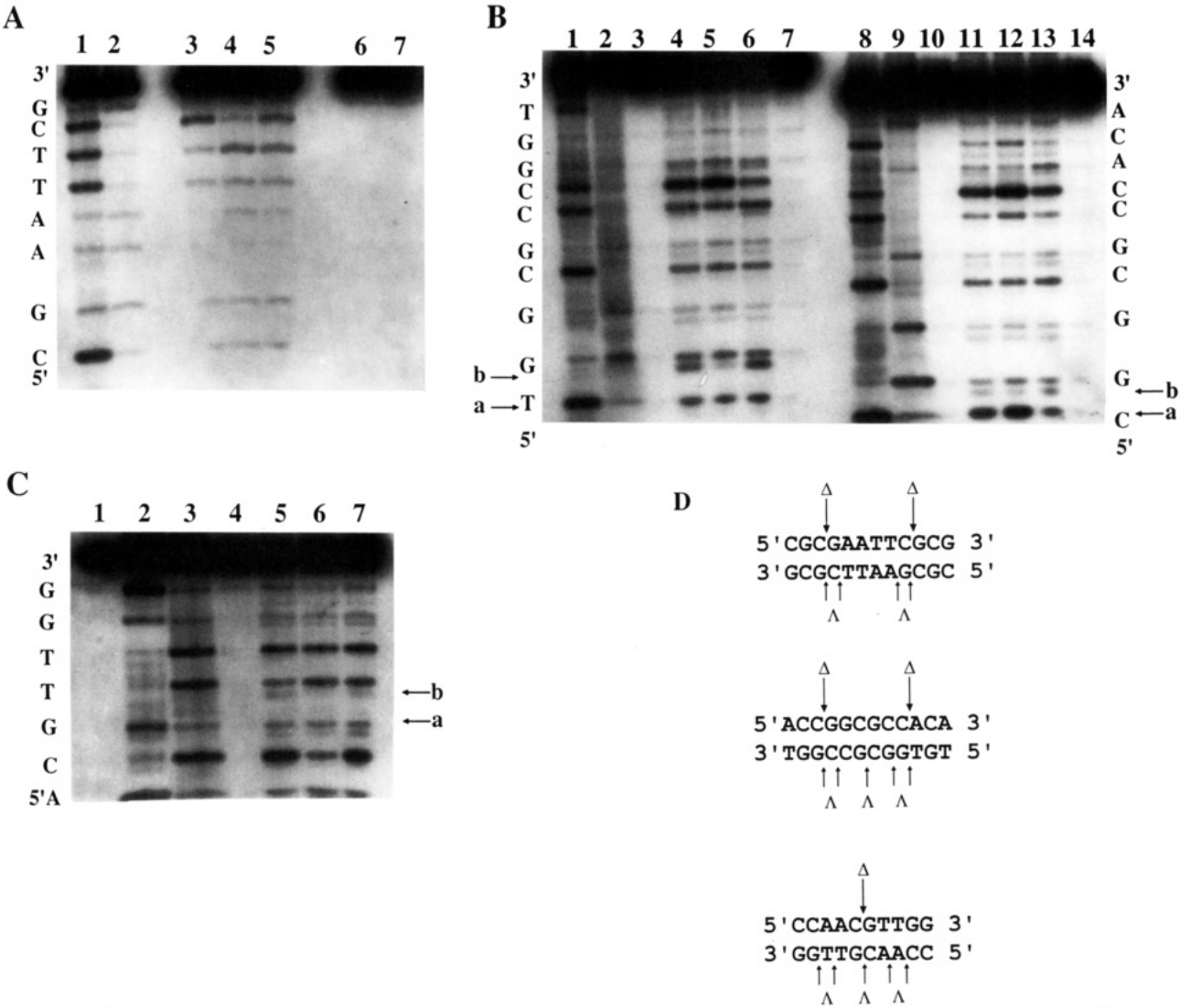

FIGURE 3: Photoinduced cleavage of 5′-^{32}P-end-labeled oligonucleotides of different sequence by the enantiomers of Rh(phen)$_2$phi^{3+}. (A) The Dickerson–Drew dodecamer. Lanes 1 and 2 are Maxam–Gilbert C + T and G + A reactions, respectively. Lanes 3, 4, and 5 show the oligonucleotide (480 μM nucleotides) after being irradiated for 1 min at 313 nm in the presence of Δ, Λ, and racemic Rh(phen)$_2$phi^{3+}, respectively. Lane 6 shows the oligonucleotide in the absence of metal complex but with irradiation and lane 7 in the absence of metal complex and without irradiation. (B) The *Nar* I dodecamer, showing cleavage on both strand 1 (left) and strand 2 (right). Lanes 1 and 8 as well as 2 and 9 are C + T and A + G Maxam–Gilbert reactions, respectively. Lanes 3 and 10 show labeled oligonucleotide without irradiation or metal complex. Lanes 4, 5, and 6 and lanes 11, 12, and 13 show the oligonucleotide irradiated for 4.5 min in the presence of racemic, Δ, and Λ Rh (phen)$_2$phi^{3+}, respectively. Lanes 7 and 14 show the oligonucleotide irradiated in the absence of metal complex. The fragments indicated by a and b correspond to the 3′-phosphate and 3′-phosphoglycaldehyde terminus, respectively; note that b shows slower mobility than its corresponding 3′-phosphate. (C) the CG decamer. Lane 1 shows the oligonucleotide in the absence of light and metal complex. Lanes 2 and 3 show Maxam–Gilbert G + A and C + T reactions, respectively. Lane 4 contains the oligonucleotide after irradiation in the absence of metal, and lanes 5, 6, and 7 show cleavage by the Δ, Λ, and racemic complexes, respectively, after irradiation for 5 min. (D) Schematic illustration summarizing sites of primary intercalation based upon cleavage data for Δ- and Λ-Rh(phen)$_2$phi^{3+}.

Thus, the strong differential propeller twist at this site in the crystal may not represent the structure in solution based upon the data presented here. Supportive evidence for this idea may be found in the crystallographic structures recently reported by Lipanov et al. (1993) for the oligonucleotide 5′-CCAACITGG-3′. This sequence crystallized both with a monoclinic packing and a trigonal packing similar, though not identical, to that found in the *Nar* I crystal structure. Significant (ca. 6°) differences in propeller twisting were found between the two packing forms.

Parallel results are observed in plots of enantioselectivity versus differential propeller twist relative to Δ cleavage versus differential propeller twist (data not shown). Since Λ-Rh(phen)$_2$phi^{3+} does not produce significantly strong sites on any of the oligomers, relative to Δ, the same correlation pertains. Plots of enantioselectivity, however, contain higher uncertainty at weak cleavage sites (positive values of x_p), since ratios between small values are required.

Correlation of Cleavage with Other Helical Parameters

We considered that other parameters which describe the structure of a base step may show some correlation with cleavage by Rh(phen)$_2$phi^{3+}. Such parameters include helical twist, rise, tilt, and roll. A weak correlation was found between helical twist values and enantioselectivity. For two of the three oligonucleotides examined, there was a direct correlation obtained between the two values, consistent with the right-handed helicity of the duplex (Barton, 1986). However, for the Dickerson–Drew dodecamer, this correlation did not hold. There was also no significant correlation found between Δ cleavage, enantioselectivity, or Λ cleavage with any of the followng: rise, tilt, groove width (phosphate–phosphate

Table 1: Quantitation of Photoinduced Cleavage by $Rh(phen)_2phi^{3+}$ on Different Oligonucleotides[a]

Dickerson–Drew			*Nar* I sequence		Δ		Λ		CG		
sequence	Δ	Λ	1	2	1	2	1	2	sequence	Δ	Λ
C3	0.11	0.07	C3	G22	1.11	0.31	0.19	0.15	A3	0.06	0.12
G4	0.12	0.08	G4	C21	0.22	1.86	0.12	0.26	A4	0.15	0.25
A5	0.05	0.06	G5	C20	0.11	0.33	0.06	0.20	C5	2.05	0.32
A6	0.05	0.07	C6	G19	0.27	0.10	0.20	0.09	G6	0.22	0.17
T7	0.22	0.14	G7	C18	0.10	0.27	0.07	0.18	T7	0.23	0.44
T8	0.31	0.32	C8	G17	0.25	0.11	0.09	0.06	T8	0.68	0.56
C9	2.54	0.25	C9	G16	2.12	0.32	0.40	0.21			
G10	0.61	0.23	A10	T15	0.27	0.26	0.25	0.33			

[a] Data are derived from gel analyses of the oligonucleotides photocleaved by $Rh(phen)_2phi^{3+}$ as shown in Figure 3. Phosphorimagery was used to determine relative band intensities for each base, and values were corrected for differences in loading and any slight damage due to light alone as described in the text. Each value shown represents the percentage cleavage on the fragment as an average of several trials. Deviations in cleavage intensity between trails were <6% for intermediate and strong sites.

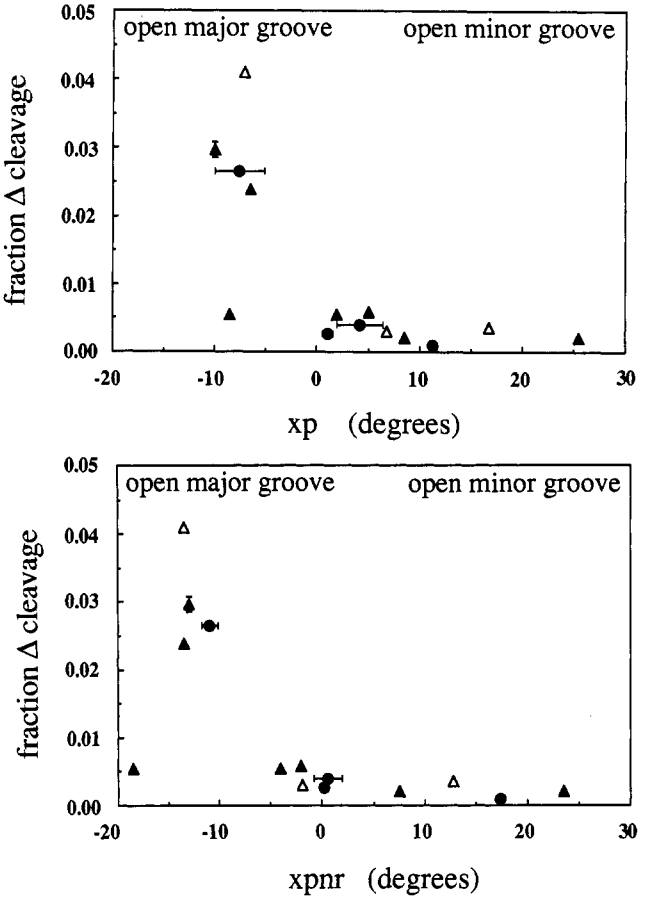

FIGURE 4: Plots showing the correlation between the percentage cleavage by Δ-$Rh(phen)_2phi^{3+}$ and differential propeller twisting corrected for roll angle (top, x_p) and without inclusion of roll angle (bottom, $x_p$nr). Data are shown for cleavage on the Dickerson–Drew dodecamer (●), the *Nar* I dodecamer (▲), and the CG decamer (△). Cleavage was quantitated at each site as described in Materials and Methods. The differential propeller twisting was determined based upon the crystallographically determined atomic coordinates [Dickerson & Drew (1981), Tismit et al. (1989), Privé et al. (1990)]. Errors for cleavage intensity are represented by the standard deviations between experiments.

distances), or roll (in isolation). This lack of correlation may arise because none of these parameters contain a symmetry axis along the dyad, except the helical twist.

Enantioselectivity in Cleavage Photoproducts

In addition to cleavage position and cleavage asymmetry, the cleavage product distribution observed as a function of

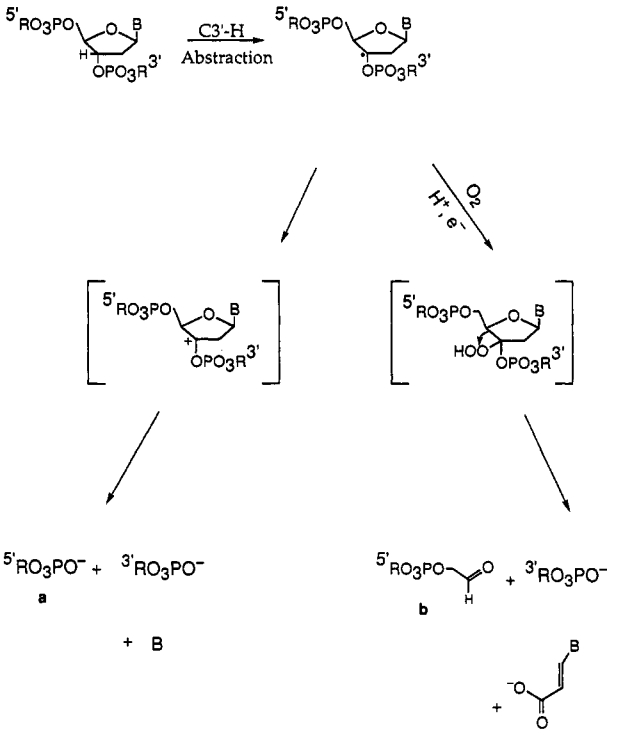

FIGURE 5: Summary of the different photoproducts obtained after partitioning along the O_2-independent and O_2-dependent pathways for strand cleavage following C3′-H abstraction.

sequence gives some insight into the interactions of these enantiomers with DNA. As described earlier (Sitlani et al., 1992) and schematically represented in Figure 5, oligonucleotide photocleavage by $Rh(phen)_2phi^{3+}$ through an O_2-independent pathway yields 5′- and 3′-phosphate termini, whereas the O_2-dependent pathway produces 5′-phosphate and 3′-phosphoglycaldehyde ends. The termini may be differentiated using gel electrophoresis, as shown in Figure 3. Hence, information may also be obtained regarding the sequence-dependence in partitioning along these pathways. Since a close shape-complementarity between the complex and the base step would block oxygen access to the C3′-radical for subsequent reaction, a high concentration of oxygen-dependent product may reflect a poor fit of the metal complex into the site.

The reaction pathway partitioning is indeed found to be sequence-dependent. In general, at a given site, the Λ enantiomer produces a greater concentration of oxygen-dependent photoproduct than does the Δ enantiomer, likely reflecting the poorer match of the left-handed isomer into the

Table 2: Quantitative Comparison of Products Obtained as a Result of Partitioning between Reaction Pathways[a]

oligomer	site	product	Δ[b]	Λ[b]	product[c] Δ	product[c] Λ
Nar I	5′-$T_{15}G_{16}$-3′	5′-RO_3PO^-	0.21	0.20	81	59
		5′-RO_3POCH_2CHO	0.05	0.14	19	41
	3′-$A_{10}C_9$-5′	5′-RO_3PO^-	2.08	0.38	98	95
		5′-RO_3POCH_2CHO	0.04	0.02	2	5
CG decamer	5′-G_6T_7-3′	5′-RO_3PO^-	0.14	0.13	61	76
		5′-RO_3POCH_2CHO	0.09	0.04	39	24
	3′-C_5A_4-5′	5′-RO_3PO^-	0.15	0.25	100	100
		5′-RO_3POCH_2CHO	0	0	0	0

[a] Data obtained in the same fashion as data from Table 1. Quantitation refers to the products formed at italicized bases. [b] Cleavage intensities shown represent the percentage cleavage on the fragment. [c] Values represent the percentage partitioning along either pathway, based upon the relative amount of product formed.

right-handed helix (Barton, 1986). The presence of oxygen-dependent photoproducts also correlates with the asymmetry in cleavage on the duplex, suggesting that canting of the complex in the helix to one strand allows oxygen access on the other.

Two illustrative examples from different oligonucleotides are shown in Table 2, and the products obtained are evident in Figure 3. These sites both show a high intensity of 3′-phosphoglycaldehyde product, but one site represents an example of high cleavage overall and the other of low cleavage. In both cases, there is little or no O_2-dependent photoproduct detected for one strand and a significant amount of phosphoglycaldehyde for the complementary strand; for a given base step, the greater the intensity of cleavage, the lower the concentration of phosphoglycaldehyde. Additionally, quantitative, sequence-dependent differences in reaction pathway partitioning are observed between enantiomers. In the 5′-$T_{15}G_{16}$-3′·5′-C_9A_{10}-3′ step from the *Nar* I dodecamer, neither enantiomer shows a significant amount of phosphoglycaldehyde at C_9, which shows the greater amount of cleavage at this base step. However, on the complementary strand T_{15}, both enantiomers show some reaction via this oxygen-dependent pathway. In fact, a greater percent of the total cleavage by Λ-Rh(phen)$_2$phi^{3+} for this 5′-YR-3′ step is found to be by this oxygen-dependent pathway, as can be seen in Table 2. Also, at the 5′-G_6T_7-3′·5′-A_4C_5-3′ step from the CG decamer, cleavage at A_4 occurs predominantly by the O_2-independent pathway for both enantiomers. However, both enantiomers show cleavage by the O_2-dependent pathway at G_6. Indeed, as can be seen in Table 2, now a greater proportion of the total cleavage by Δ-Rh(phen)$_2$phi^{3+} occurs via the oxygen-dependent pathway at this base. Thus, while the 5′-RY-3′ step does not prove to be a suitable binding site for either enantiomer, the fit at this site tends to be worse for Δ than for Λ. (This observation may be rationalized by steric clashes between the 2,9 hydrogens of the phenanthroline and the functional groups on the purine bases in the major groove.) Furthermore, the generally low cleavage at these sites is to be expected since they are closed in the major groove (*vide supra*).

The relative amount of phosphoglycaldehyde photoproduct at a particular site can therefore serve as an indicator of the accessibility of dioxygen to that site and thus of the fit between the shape of the metal complex and the shape of that site. The sequence dependence in photoproducts observed in summarized in Table 3 and may be generally considered in that context.

Table 3: Summary of Sequence-Dependent Photoproducts Observed in Reaction with Rh(phen)$_2$phi^{3+} Enantiomers[a]

sequence	overall intensity of cleavage	enantio-selectivity in cleavage	enantioselectivity in formation of O_2-dependent products
5′-YYRN-3′	high	Δ ≫ Λ	Λ > Δ
5′-RYRN-3′	intermediate	Δ ≥ Λ	Λ > Δ
5′-NYYN-3′[b] and 5′-NRRN-3′	intermediate	Δ ~ Λ	Λ > Δ
5′-NRYN-3′	low	Δ ~ Λ	sequence-dependent[c]

[a] Comparisons refer to reaction at the italicized bases. [b] Except 5′-GYYN-3′. [c] For some sequences there is too little product for detection.

DISCUSSION

Major Groove Intercalation. The features which govern DNA recognition by Rh(phen)$_2$phi^{3+} determine both its binding and cleavage characteristics. Strong sites of cleavage often display single base 5′-asymmetry, consistent with binding from the major groove (Dervan, 1986). In the case of Rh(phen)$_2$phi^{3+}, with asymmetric binding, one furthermore observes the production of 3′-phosphoglycaldehyde termini, a cleavage product consistent with reaction at the C3′ hydrogen atom in the major groove. The fact that the complex binds by intercalation from the major groove (David & Barton, 1993; Sitlani et al., 1992) importantly differentiates the complex from many natural products and chemical probes which bind the DNA duplex in the minor groove (Sigman, 1986; Saito et al., 1989; Lomonosaff et al., 1981). This contrast becomes evident in comparing probes on the Dickerson–Drew dodecamer. Δ-Rh(phen)$_2$phi^{3+} cleaves mainly at C_9, which corresponds to binding at the C_9G_{10} step. The Λ enantiomer binds and cleaves at the T_8C_9 and the C_9G_{10} step. Each differs from the minor-groove binding Cu(phen)$_2^+$, which cleaves at all positions of this oligonucleotide (Sigman, 1986), and the green bleomycin–cobalt(III) complex, which cleaves predominately at the C_3 and C_{11} positions (Saito et al., 1989). These complexes also differ in distribution of cleavage from minor groove binding DNase I (Lomonossaff et al., 1981) which cleaves strongly at T_8.

Each step which is cleaved strongly by Δ-Rh(phen)$_2$phi^{3+} is a 5′-NYRN-3′ step. This step is thought to be favorable for classical intercalators (Krugh & Reinhardt, 1975) because of the stability which may be gained by overlap with the intercalator. Although intercalation has been demonstrated as the primary binding mode for this complex (David & Barton, 1993), the chiral discrimination at all sites, favoring the Δ isomer, also shows that this intercalative overlap with the base pairs is not the sole factor governing site recognition. In other words, the disposition of the ancillary phenanthroline ligands about the metal center provides another structural element in distinguishing one site from another. The feature being discerned by means of steric repulsion on the helix is, likely, the angle of opening of the purines toward the major groove.

Enantioselectivity in Rh(phen)$_2$phi^{3+}–DNA Interactions. The following all give information about the differences in

interaction between the enantiomers of this complex and a given site: total intensity of cleavage, cleavage asymmetry, and mechanistic partitioning of the photoproducts. As may be seen in Tables 1 and 2 and summarized in Table 3, the greatest difference in total cleavage between the enantiomers is at 5′-YR-3′ steps, in particular 5′-YYRN-3′ steps. Enantioselectivity (Δ cleavage/Λ cleavage) of up to a factor of 10 has been observed for these steps, particularly when flanked by a 5′-pyrimidine. The Δ enantiomer also shows a greater degree of cleavage asymmetry at 5′-YR-3′ steps than does the Λ enantiomer. This asymmetry is dependent on neighboring bases as well. If only one base in the base step possesses a 5′ flanking pyrimidine, cleavage is weighted toward that side for *both* enantiomers, but the asymmetry is more dramatic for the Λ enantiomer. While asymmetric intercalation has also been demonstrated in crystal structures (Sakore et al., 1977) of some planar intercalators bound to 5′-CG-3′ dinucleotide steps, this work shows that flanks may influence the local structure and recognition of 5′-YR-3′ steps. Again, the disposition of the ancillary phenanthrolines is likely to enhance the discrimination.

The enantiomers also show differences in how cleavage products are partitioned along the two pathways. The amount of O_2-dependent photoproducts, along with asymmetry of cleavage, gives information as to the fit of the bound molecule in the site, the shape-complementarity of the metal complex to the local structure of DNA. For example, as shown in Table 3, at the 5′-YYRN-3′ and 5′-RYRN-3′ steps, it is the Δ enantiomer which yields a relatively small amount of phosphoglycaldehyde terminus, and which thus has the better fit for this site. The better fit of the Δ-isomer in most sites is evident, based upon this criterion, including 5′-GC-3′ steps. At low sites of cleavage, where neither enantiomer likely fits well, both isomers may yield O_2-dependent products; indeed at the A_4C_5 step of the CG decamer, the Δ-isomer yields more 3′-phosphoglycaldehyde. It should be noted that at some sites the total cleavage is so low that no O_2-dependent photoproduct is detectable. These cases suggest the worst fit between enantiomers and the site, with substantial steric clashes between the ancillary ligands and the bases.

Recognition Structure. What then are the structural features of DNA which are being distinguished by Δ-Rh(phen)$_2$phi^{3+}? It may be said that this complex is recognizing groove width in a coarse fashion. Rh(phen)$_2$phi^{3+} specifically cleaves B-form DNA or other nucleic acid structures where the major groove is open enough to allow binding. On the other hand, the rhodium complex does not cleave the double-helical regions of tRNA (Chow et al., 1992a) because the narrow major groove precludes binding by the complex. Thus, the first determinant of the "open major groove" is a groove possessing a width large enough to accommodate the complex. From comparisons with groove widths obtained from coordinates of the Dickerson–Drew dodecamer and the CG decamer, however, it does not appear that the complex is recognizing small variations in groove width within the range evident in the B conformation. There are two possible explanations for this. Crystal packing affects groove width values more than it does most other parameters. Differences dependent on packing have been observed for the B conformation (Lipanov et al., 1993) and the A conformation (Shakked et al., 1989; Jain & Sundaralingam, 1989; Ramakrishnan & Sundaralingam, 1993). Therefore, small variations in groove widths in crystal structures may not be wholly indicative of the solution structure. Alternatively, the binding characteristics of Rh(phen)$_2$phi^{3+}, an intercalator rather than a large groove binding molecule, do not lend themselves to subtle comparisons with variations in groove width.

A related aspect is the inclination of the base pairs with respect to one another, the base pair tilt. While it does not appear that the complex is recognizing tilt in a strictly quantitative fashion, all of the strong cleavage sites for the Δ enantiomer in these oligonucleotides possess a tilt angle which is less than or equal to zero. It also does not appear that tilt correlates with the asymmetry of the cleavage.

Other parameters can define openings in the major groove. Although it had been suggested (Calladine, 1982) that sequence could dictate opening toward or away from the major groove through variations strictly in the roll angle, cleavage by neither enantiomer nor enantioselectivity in cleavage by Rh(phen)$_2$phi^{3+} correlate with the roll angle in isolation. There also does not appear to be a correlation between cleavage by either enantiomer and the sequence-dependent rise of a base step. As this rise is determined by the C1′–C1′ distance in a step, it would be surprising to find this parameter to be sensitive to considerations of intercalator chirality.

However, one parameter which might be expected to govern enantioselectivity in cleavage is the helical twist. Although there is a weak direct correlation between the two sets of values, it only holds for the *Nar* I dodecamer and the CG decamer; it does not hold for the Dickerson–Drew dodecamer. The explanation for this may lie in the high twist profile (HTP) and low twist profile (LTP) described by Yanagi et al. (1991). The HTP describes steps having a high twist, low rise, and negative roll, whereas the LTP describes steps having a low twist, large rise, and positive roll. The 5′-YR-3′ step has been shown from a body of crystallographic structures (Yanagi et al., 1991) and calculations (Hunter, 1993) to exhibit both types of behavior. Correlations made which factor in helical twist, roll, and rise are not straightforward. Thus, although helical twist is not explicitly accounted for in the calculation of the differential propeller twisting, it may contribute in part to the resultant enantioselectivity in cleavage. The correlation of overall helix chirality with enantioselectivity has been demonstrated for metallointercalators, groove binding agents, and complexes which coordinate directly to the helix (Barton, 1986).

What the Δ enantiomer locally appears to recognize is the rotation of the base pairs about their long axes, e.g., the angle between the purine planes caused by the propeller twisting of the base pairs as defined in Figure 2. Rh(phen)$_2$phi^{3+} is therefore unique in recognizing an important element in DNA local structure. Both propeller twist angles and the roll angle contribute to this parameter, which also may be considered as a measure of the major groove opening of DNA. As Figure 4 reveals, *there is a strong correlation between the intensity of cleavage of Δ-Rh(phen)$_2$phi^{3+} at a site and the degree of openness in the major groove as a result of sequence-dependent base pair propeller twisting.* The sign of this parameter shows opening (negative) or closing (positive) of the major groove, in the same convention as the roll angle. The extent of the opening may be approximated by the values of the parameter. Importantly, it is not the propeller twist itself which is recognized by the metal complex, but instead *the change* in propeller twist. Sites of substantially enantioselective cleavage are observed both where there is a 26° propeller at one base pair and 0° at the next (in the C_3G_4 base step of *Nar* I) and where the angle is 13° at one base pair and 14° at the next (in the C_9A_{10} base step of *Nar* I). Both geometries lead to sites which are open in the major groove.

In order to test the contribution of the roll angle to this opening, $x_p$nr, the differential propeller twisting without inclusion of the roll angle, was also calculated. While the general agreement between enantioselectivity and differential propeller twisting still holds, it does not appear to correlate as well as when the roll angle is included. Particularly, there are two sites (C_3 and C_9 of the *Nar* I dodecamer) which show the same $x_p$nr, but quite different cleavage values. It should be noted that neither x_p nor $x_p$nr correlates with the corresponding roll angle alone.

It is also interesting to compare these cleavage results to structural parameters obtained for these oligonucleotides in solution by NMR. Such a comparison may be drawn in particular in the case of the Dickerson–Drew dodecamer where several laboratories have carried out relevant NMR experiments (Pardi et al., 1988; Kaluarachchi et al., 1991; Nerdal et al., 1989). In one case (Nerdal et al., 1989), NMR analysis revealed a more substantial kink at the C_3G_4 base step, the site of strongest cleavage by Δ-Rh(phen)$_2$phi^{3+}, than is evident in the crystal, indeed a structural kink similar to that found in the crystal with bound *Eco*RI (McClarin et al., 1986). Other analyses show general agreement between the structure in the crystal and in solution but emphasize that propeller twisting is among the inherently least well-determined parameters available by NMR (Paerdi et al., 1988). In the case of the CG decamer, solution NMR analysis has also been performed and compared to the crystal structure (Nibedita et al., 1992). Here while detailed structural parameters are not available, general agreement between the solution and crystal structure appears to be found. Hence, in both these cases correlations appear to be present between site-specific cleavage by the rhodium complex with solution as well as crystallographically determined oligonucleotide structure.

Biological Relevance. It has been demonstrated that Rh(phen)$_2$phi^{3+} recognizes a particular structural feature of DNA. Does this recognition have any relevance to protein–nucleic acid recognition? Binding by the Δ enantiomer shows several similarities to that of many sequence-specific DNA-binding proteins. Firstly, both bind primarily from the major groove and are therefore sensitive to major groove structure. Secondarly, both bind through a hierarchy of noncovalent interactions. In the case of the metal complex, the primary driving force is intercalation, but the ancillary ligands modulate site recognition, primarily through steric considerations. In the case of DNA-binding proteins, often nonspecific electrostatic interactions provide a substantial driving force for binding to the nucleic acid. Flanking sequences can also affect binding specificity either directly or by altering the local shape of the site. For example, in this set of data, having a guanine to the 5′ side strongly reduces the affinity of the complex for a 5′-CG-3′ step. Likewise, flanks (Drew & Travers, 1985; Koudelka et al., 1987) can reduce/increase protein binding affinity to particular sites.

Another similarity rests in the ability of both the complex and some proteins to change the structure of DNA upon binding. Rh(phen)$_2$phi^{3+} necessarily deforms every site to which it binds due to its intercalation. Proteins as well can cause changes in the B-form structure upon binding. For example, in the cocrystal (McClarin et al., 1986) of *Eco*RI with its recognition sequence, the Dickerson–Drew dodecamer, the sequence 5′-TCG-3′ shows a kink, which increases the phosphate–phosphate distance between residue C_9 and G_{10}, and of particular interest, the propller twist of the C_3 and G_{10} steps. This structure is not observed in the DNA crystal lacking the protein, but as described above, a similar kink may be apparent in solution in the absence of protein (Nerdal et al., 1989) and may influence binding both by protein and Rh(phen)$_2$phi^{3+}. The cocrystal (Somers & Phillips, 1992) of the *met* repressor–operator complex shows that the central CG step exhibits a conformation altered from the B-form, and changes in this step affect the binding affinity of the *met* repressor (Phillips et al., 1989). It is interesting that in this case and in that of *Eco*RI, Rh(phen)$_2$phi^{3+} appears to be cleaving at sites whose structures are perturbed by protein binding.

More generally, there are similarities between the actual sequences recognized by Rh(phen)$_2$phi^{3+} and those recognized by some proteins. One site which is cleaved very strongly by Δ-Rh(phen)$_2$phi^{3+}, which is not a 5′-YYRN-3′ step, is the 5′-AC$_5$G$_6$T-3′ of the CG oligonucleotide. This sequence appears to be particularly prevalent in transcription factor binding sites. These include, for example, the ATF promoter (Hai et al. 1989). 5′-ACGT-3′ is also part of the recognition sequence for the *met* repressor (Phillips et al., 1989). Another group of sites are the recognition sequences for the TFIIIA family of zinc fingers. A recent crystal structure of five-finger GLI with a 21-mer (Pavletich & Pabo, 1993) shows two fingers which are bound most closely in the opened major groove containing 5′-CCAC-3′, a sequence also contained in the *Nar* I dodecamer, and which is recognized by Rh(phen)$_2$phi^{3+}. The general correspondence of cleavage sites with protein recognition sites may reflect the importance of an open major groove for binding by a family of proteins (Huber et al., 1991). A structure which is open in the major groove may serve as a landmark for the binding of proteins and small molecules alike. This correlation of sites recognized by Rh(phen)$_2$phi^{3+} with protein binding is particularly striking in the case of 5S RNA (Chow et al., 1992b).

A related question is whether Rh(phen)$_2$phi^{3+} is recognizing sequence-dependent structure or sequence-dependent deformability. The fact that correlations have been found between cleavage and structures which have been crystallized *without metal complex* offers support to the notion that the structure which is present in the DNA before binding by the metal complex correlates well with the strength of the metal complex–DNA interaction after binding. The enantioselective discrimination at these sites also suggests structural recognition as a predominant signal. Indeed, the strong correlation found between cleavage at sites with a large differential propeller twist rather than, for example, at the ends of the oligonucleotide helix, irrespective of sequence, suggests that transient openings in the helix are insufficient for site-specific cleavage. Nonetheless, just as with DNA–protein binding, the recognition of sequence-dependent structure and of sequence-dependent deformability are difficult to unravel. Here, too, the deformability of a particular sequence toward a more opened propeller-twisted state may be one feature of site-recognition.

CONCLUSION

Therefore, in direct comparisons of cleavage by Rh(phen)$_2$phi^{3+} with different, crystallographically characterized oligonucleotides, we have determined factors which govern sequence-selective recognition by Rh(phen)$_2$phi^{3+}. Both binding and reaction at sites are governed by considerations of shape and symmetry. In particular, enantioselective cleavage favored by the Δ-isomer is governed locally by the opening of the site in the major groove. The change in base pair propeller twisting of the site correlates most closely with recognition by Δ-Rh(phen)$_2$phi^{3+}. Hence, these results provide support for site-recognition which depends upon DNA

propeller twisting in solution. Therefore, these results indicate that $Rh(phen)_2phi^{3+}$ may be uniquely and powerfully applied as a chemical probe for sequence-dependent propeller twisting of DNA.

ACKNOWLEDGMENT

We thank S. David for providing enantiomerically pure rhodium complexes.

REFERENCES

Barton, J. K. (1986) *Science 233*, 727–732.
Calladine, C. R. (1982) *J. Mol. Biol 161*, 343–352.
Caruthers, M. H., Barone, A. D., Beaucage, S. L., Dodds, D. R., Fisher, E. F., Mc Bride, L. J., Matteucci, M., Stabinsky, Z., & Tang, J.-Y. (1987) *Methods Enzymol. 154*, 287–313.
Chow, C. S.; & Barton, J. K. (1992) *Methods Enzymol. 212*, 219–242.
Chow, C. S., Behlen, L. S., Uhlenbeck, O., & Barton, J. K. (1992a) *Biochemistry 31*, 972–982.
Chow, C. S., Hartmann, K. M., Rawlings, S. L., Huber, P. W., & Barton, J. K. (1992b) *Biochemistry 31*, 3534–3542.
David, S. D., & Barton, J. K. (1993) *J. Am. Chem Soc. 115*, 2984–2985.
Dervan, P. B. (1986) *Science 232*, 464–471.
Dickerson, R. E., & Drew, H. (1981) *J. Mol. Biol. 149*, 761–786.
Drew, H. R., & Travers, A. A. (1985) *Nuc. Acids Res. 13*, 4445–4467.
Drew, H. R., & Travers, A. A. (1984) *Cell 37*, 491–502.
Drew, H. R., McCall, M. J., & Calladine, C. R. (1990) in *DNA Topology and Its Biological Effects*, p 1–55, Cold Spring Harbor Laboratory Press, Cold Spring Harbor.
Drew, H. R., Wing, R. M., Takano, T., Broka, C., Tanaka, S., Itakura, K., & Dickerson, R. E. (1981) *Proc. Natl. Acad. Sci. U.S.A. 78*, 2179–2183.
EMBO Workshop on DNA Curvature and Bending, (1989) *EMBO J. 8*, 1–4.
Frantini, A. V., Kopka, M. L., Drew, H. R., & Dickerson, R. E. (1982) *J. Mol. Biol. 257*, 14686–14707.
Hai, T., Fang, L., Coukos, W. J., & Green, M. R. (1989) *Genes Dev. 3*, 2083–2090.
Huber, P., Morii, T., Mei, H.-Y., & Barton, J. K. (1991) *Proc. Natl. Acad. Sci. U.S.A. 88*, 801–805.
Hunter, C. A. (1993) *J. Mol. Biol. 230*, 1025–1054.
Jain, S., & Sundaralingam, M. (1989) *J. Biol. Chem. 264*, 12780–12784.
Kaluarachchi, K., Meadows, R. P., & Gorenstein, D. G. (1991) *Biochemistry 30*, 8785–8797.
Kennard, O., & Hunter, W. N. (1989) *Q. 'Rev. Biophys. 22*, 327–379.
Koudelka, G. B., Harrison, S. C., & Ptashne, M. (1987) *Nature 326*, 886–888.
Krugh, T. R., & Reinhardt, C. G. (1975) *J. Mol. Biol. 97*, 133–162.
Lipanov, A., Kopka, M. L., Kaczor-Grzeskowiak, M., Quintana, J., & Dickerson, R. E. (1993) *Biochemistry 32*, 1373–1389.
Lomonosaaf, G. P., Butler, P. J. G., & Klug, A. (1981) *J. Mol. Biol. 149*, 749–760.
Maniatis, T., Fritsch, E. F., & Sambrook, J. (1982) in *Molecular Cloning*, Cold Spring Harbor Laboratory Press, Cold Spring Harbor.
McClarin, J. A., Frederick, C. A., Wang, B.-C., Greene, P., Boyer, H. W., Grable, J., & Rosenberg, J. M. (1986) *Science 234*, 1526–1541.
Metzler, W. J., Wang, C., Kitchen, D. B., Levy, R. M., & Pardi, A. (1990) *J. Mol. Biol. 214*, 711–736.
Nerdal, W., Hare, D. R., & Reid, B. R. (1989) *Biochemistry 28*, 10008–10021.
Nibedita, R., Kumar, R. A., & Majumdar, A. (1992) *J. Biomol. NMR 2*, 477–484.
Otwinowski, Z., Scheritz, Zhang, R.-G.; Lawson, C. L., Joachimiak, A., Marmorstein, R. Q., Luisi, B. F., & Sigler, P. B. (1988) *Nature 335*, 321–329.
Pabo, C. O., & Sauer, R. T. (1992) *Annu. Rev. Biochem. 61*, 1053–95.
Pardi, A., Hare, D. R., & Wang, C. (1988) *Proc. Natl. Acad. U.S.A. 85*, 8785–8789.
Patel, D. J., Shapiro, L., & Hare, D. (1987) *Q. Rev. Biophys. 20*, 35–112.
Pavletich, N. P., & Pabo, C. O. (1993) *Science 261*, 1701–1707.
Phillips, S. E. V., Manfield, I., Parsons, I., Davidson, B. E., Rafferty, J. B., Somers, W. S., Maragarita, D., Cohen, G. N., Saint-Girons, I., & Stockley, P. G. (1989) *Nature 341*, 711–715.
Privé, G. G., Yanagi, K., & Dickerson, R. E. (1991) *J. Mol. Biol. 217*, 177–199.
Pyle, A. M., & Barton, J. K. (1990) *Prog. Inorg. Chem. 38*, 413–475.
Pyle, A. M., Morii, T., & Barton, J. K. (1990a) *J. Am. Chem. Soc. 112*, 9432–9434.
Pyle, A. M., Chiang, M., & Barton, J. K. (1990b) *Inorg. Chem. 29*, 4487–4495.
Pyle, A. M., Long, E. C., & Barton, J. K. (1989) *J. Am. Chem. Soc. 111*, 4520–4522.
Ramakrishnan, B., & Sundaralingam, M. (1993) *Biochemistry 32*, 11458–11468.
Saito, I., Morii, T., Sugiyama, H., Matsuura, T., Meares, C. F., & Hecht, S. M. (1989) *J. Am. Chem. Soc. 111*, 2307–2308.
Sakore, T. D., Jain, S. C., Tsai, C.-C., & Sobell, H. M. (1977) *Proc. Natl. Acad. Sci. U.S.A. 74*, 188–192.
Shakked, Z., Guerstein-Guzikevich, G., Eisenstein, M., Frolow, F., & Rabinovich, D. (1989) *Nature 342*, 456–460.
Sigman, D. S. (1986) *Acc. Chem. Res. 19*, 180–186.
Sitlani, A., & Barton, J. K. (1993) in *Handbook of Metal-Ligand Interactions of Biological Fluids*, Marcel-Dekker, Inc., New York.
Sitlani, A., Long, E. C., Pyle, A. M., & Barton, J. K. (1992) *J. Am. Chem. Soc. 114*, 2303–2312.
Somers, W. S., & Phillips, S. E. V. (1992) *Nature 359*, 387–393.
Steitz, T. A. (1990) *Q. Rev. Biophys. 23*, 205–280.
Stubbe, J., & Kozarich, J. W. (1987) *Chem. Rev. 87*, 1107–1136.
Timsit, Y., Westhof, E., Fuchs, R. P. P., & Moras, D. (1989) *Nature 341*, 459–462.
Tullius, T. D. (1992) *Methods Enyzmol. 212*, 219–242.
Yanagi, K., Privé, G. G., & Dickerson, R. E. (1991) *J. Mol. Biol. 217*, 201–214.